SLAC-PUB-57
October 1964

PRECISION MAGNETIC MEASUREMENTS USED FOR THE DESIGN OF THE STANFORD TWO-MILE LINEAR ACCELERATOR TRANSPORT SYSTEMS*

J. K. Cobb and J. J. Muray
Stanford Linear Accelerator Center
Stanford University, Stanford, California

Abstract

In order to utilize the electron beam of the Stanford two-mile accelerator most effectively, an elaborate beam switchyard will be used. Two basic components constitute the switchyard: a switching magnet and two deflecting transport systems. A precision deflection magnet system containing several dc magnets and quadrupoles will bend and momentum-analyze the electron and positron beams.

This paper discusses the methods and techniques used in making high-precision magnetic measurements in dc and multipole magnetic fields. The requirements for the accuracy of field measurements are deduced from the beam optics of the transport systems. Special measurements and instruments used in these measurements will be discussed in detail, and the results of these measurements will be related to the optical properties of the particle beams. Special measurements in multipole magnets, such as the location of the magnetic center, the magnetic coordinate system, multipole content, effective length, and different methods of making such measurements, will be discussed.

Introduction

The electron beam of the Stanford two-mile accelerator will be magnetically directed to various experimental areas in an elaborate beam switchyard. A schematic layout of the switchyard is shown in Fig. 1. The magnets in this switchyard will provide the 12.5° and 24.5° deflections necessary to allow the different experimental areas to be shielded and separated from each other. In addition to providing flexibility of experimental arrangements, the switchyard will assure and measure the beam energy going into the experimental areas. In this function the beam switchyard can be considered to be an energy-analyzing transport system in which the proper energy for the experiment is defined by the collimator between the accelerator and the switchyard, the bending angle in the magnetic field, and the energy-defining slit.

This paper discusses the methods and techniques used in making high-precision magnetic measurements on the various types of magnets that are used in this transport system. The requirements for the accuracy of field measurements are deduced from the optics of the whole facility including the accelerator itself.

In designing the accelerator[1] and the beam transport system,[2] the behavior of the electron beam as a whole, which is best analyzed in terms of displacement-divergence in the phase space, was very important. When the horizontal motion of the electron beam in the x and y direction is decoupled, the beam "quality" can be characterized by

$$\iint dx\, d(\gamma x') \quad \text{and} \quad \iint dy d(\gamma y')$$

at energy $E = \gamma m_o c^2$, where the integrals are the projections of the phase space to the xz and yz planes, and x' and y' are the beam divergences. It is evident from this definition that a beam of small size and angular divergence has a small phase space. In these terms then, the basic philosophy for the design of the beam transport system was to minimize the beam envelope, or the phase space, with the condition that the experimental area will get a beam with the minimum phase space and the required energy spread ($\Delta E/E$).

The expected angular spread (divergence) of the electron beam from the accelerator is

$$y', x' \leq \frac{2 \times 10^{-4}}{E(\text{BeV})}$$

This number, however, is an order of magnitude value only, because it does not take into account the effect of possible asymmetries in the rf circuit[3] for the accelerator waveguide, the possible radial electrical fields, and the misalignment[4] of the accelerator. These and other considerations, such as reducing the beam size in the accelerator, allowing for possible non-conservation of transverse phase space (scattering, collimation of the beam), suggest a focusing system for the accelerator which produces a radial focusing of the beam somewhat stronger than the minimal requirement for electron transmission.

The actual strong focusing magnet system consists of quadrupole triplets spaced every 300 feet along the accelerator.[5] These triplets form a periodic focusing system analogous to a periodic focusing system of thin lenses in the case of a light beam. The alignment of the quadrupole axis should be stable to within 0.001 inch rms relative to the mean reference axis of the triplet. Also spaced at 300-foot intervals along the accelerator are small dipoles which will continuously make minor corrections in the beam position and direction.

The maximum beam radius out of the accelerator is expected to be $a = 0.4$ cm. The radial current density distribution in the beam will not

*Work supported by the U. S. Atomic Energy Commission.

(Paper presented at the 11th annual Nuclear Science Symposium, IEEE Transactions on Nuclear Science, Philadelphia, Pennsylvania, October 28-30, 1964.)

have a sharp cut-off, but rather a gaussian distribution

$$j = j_o e^{-\frac{1}{2}(r/a)^2}$$

which gives $I_o = 2\pi a^2 j_{max}$. With $I_o = 120\ \mu A$, the maximum beam current density is $860\ \mu A/cm^2$.

The electron beam from the accelerator will go through a collimator to assure the proper beam alignment to the switchyard. However, the collimator will probably increase the angular divergence of the beam. If the hole in the collimator has a radius r = 0.3 cm, 86.5% of the beam will go through unaffected, but most of the remainder of the beam will come out with energies ranging from zero to almost full energy and with a divergence up to 10^{-3} radian. After a distance of 80 meters (at the first pair of quadrupoles), the beam profile's 2-cm-width will be superimposed on the scattered beam which will have a width of $\approx$ 10 cm. The bending magnets will have a "homogeneous" field of about 6.5 cm in width, the quality of which should be such that the image size (collimator hole) is not enlarged by aberrations at the position of the energy slit. This requires that the difference in deflection angle between the central 2-cm beam and the outermost part of the scattered beam should be small compared to the angle at which the collimator is seen from the bending magnets. This gives a tolerance for the field homogeneity in the gap, namely,

$$\frac{\Delta B}{B_o} \ll \frac{r}{\ell\varphi}$$

With the deflection angle $\varphi = 12^o$, r = 0.3 cm and ℓ = 80 meters; this gives

$$\frac{\Delta B}{B_o} \ll 2 \times 10^{-4}$$

The opening of the energy-defining slit determines the energy spectrum of the electron beam sent to the experimental area.

Magnets in the Transport System

In the beam transport system, including the accelerator itself, three different kinds of magnets are used: dc bending magnets, pulsed deflection magnets, and quadrupole magnets.

The dc bending magnets are used to deflect and momentum-analyze the electron beam coming from the accelerator. The geometry of a bending magnet which deflects the central trajectory through an angle α is shown in Fig. 2. The central trajectory is that path which has the coordinates $x = 0$, $x' = 0$ in the horizontal plane, and a central momentum $P_o = qrB$. When the input beam is characterized by x_o displacement, x_o' divergence, and $\Delta p/p$ momentum spread, the output beam parameters after deflection through an angle α can be written in a matrix form[6] when the input beam is perpendicular to the entrance edge at the pole face ($\beta_1 = 0$) as shown in the matrix equation at the bottom of this page. In this equation, $\alpha r = s$, where s is the section of the particle trajectory within the magnetic field (including the fringing field of the magnet). A similar expression[6] can be written for the transformation matrix in the vertical direction. Due to the edge effect of the magnet, the beam is deflected vertically at the edges. This vertical deflection has the effect of focusing the beam and can be expressed as a thin focusing lens with focal distance.

$$f = \frac{r}{\tan \alpha/2}$$

To calculate the trajectory in an inhomogeneous magnetic field, one can approximate the particle orbit by a succession of circular arcs. The angle of deflection of any point s_o is

$$\alpha_{s_o} = \frac{\int_{s_n'}^{s_{n+1}} B\,ds}{Br} \qquad \text{where} \quad n = 1, \ldots, N$$

$$\begin{pmatrix} x \\ x' \\ \frac{\Delta p}{p} \end{pmatrix} = \begin{pmatrix} \cos\alpha & r\sin\alpha & r(1-\cos\alpha) \\ \frac{-(1-\tan\beta_2)\sin(\alpha-\beta_2)}{r\cos\beta_2} & \frac{\cos(\alpha-\beta_2)}{\cos\beta_2} & \sin\alpha + (1-\cos\alpha)\tan\beta_2 \\ 0 & 0 & 1 \end{pmatrix} \begin{pmatrix} x_o \\ x_o' \\ \frac{\Delta p}{p} \end{pmatrix}$$

Then, using the α_{s_o}'s, and the corresponding r's in the N transformation matrix, the beam parameters can be calculated when N steps were taken. This can be done when

$$\int_{s_n}^{s_{n+1}} Bds$$

is known for each arc from s_n to s_{n+1} along the particle trajectory.

For beam trajectory calculations, quantities like

$$\int_{s_n}^{s_{n+1}} Bds$$

are measured by using point measurements in the magnet and calculating the integral numerically. In certain cases the integral quantity can be measured directly.

In making point measurements one can use the usual methods and sensors to map the magnetic field. Depending on the accuracy required, different field sensors can be used. Table I lists the different field measuring instruments and their characteristic properties. By using an integrating measuring device such as a rotating long coil through the magnet and by integrating the induced voltage from the coil, one can measure the effective length of the magnet, which is defined by

$$\ell_{eff} = \frac{\int Bds}{B_{max}}$$

Here B_{max} is the maximum field and the integral is to be taken over a straight line through the magnet aperture. This is a very good approximation of a particle trajectory when the deflection angle α is small, i.e., when $\alpha\ell < d$ where ℓ is the length of the coil and d is the diameter of the rotating coil.

Because a large number of measurements are required for the beam switchyard bending magnets, a special device was designed[7] to measure the field in the gap along an actual particle trajectory. An aluminum guide beam capable of being bent to a circular arc is placed in the magnet. It is held in the circular arc by clamping to aluminum angle brackets fastened to the magnet end covers (magnetic mirrors). On the aluminum guide beam an aluminum carriage holding the sensor and flip device is driven by an integrally mounted brass lead screw contained by plastic guide pieces. The lead screw is driven by a reversible air motor capable of driving the carriage from 0 to 20 inches/minute.

Two types of flip devices have been designed. One makes use of two parallel non-magnetic pneumatic cylinders driving a linear cam, which rotates the shaft on which the sensor coil is mounted through 180°. The other type makes use of a reversible air motor which is rotated through 180° and is positioned by shaft-mounted stops.

Position readout is accomplished by means of a Veedor-Root counter that is coupled to the lead screw. A small position error is introduced because the lead screw follows the bent guide beam, the length of which is slightly greater than the coordinate line drawn from the sensor to the driving device.

Figure 3 shows the 3° bending magnet positioner. This device has proved most useful in transporting other sensing devices (NMR probes and Hall probes) through the magnet longitudinally for high precision measurements.

The homogeneity in the bending magnet can be measured, using a long coil and integrator, as a function of the transverse (x) position across the magnet gap. The accuracy of this measurement is about ±1 part in 10^5, and it is limited by the mechanical design of the coil and coil turning mechanism and by the accuracy of the integrator. Figure 4 shows the 4-meter-long rotating coil and its turning mechanism; Fig. 5 is a photograph of the whole measuring setup showing the integrator (Dymec 2401B), the printer (Hewlett Packard, Model H25562A), and the coil rotating motor.

Field Measurements in Pulsed Magnetic Fields

The measurement of time-varying or pulsed magnetic fields involves techniques different from those used for static fields. In making dynamical field measurements, the measuring instrument should give a signal which is an instantaneous measure of the field and is not influenced by the eddy-current fields in the measuring probe.

To measure the magnetic field in the pulsed deflection magnet, an electron magnetic resonance device,[8] using DPPH as an organic free radical, was chosen. DPPH has a linewidth of 1.35 gauss, a relaxation time of about 0.2 μsec, and a g-value of 2.0036 ± 0.0002. With the g-value of DPPH, the resonance frequency is given by F = (2.804 ± 0.001)B, where F is the frequency in Mc and B_o is the field in gauss. Therefore, fields of 1400 to 2100 gauss will resonate with microwave signals from 3.95 to 5.85 k Mc, the "G" band region.

A helix slow wave structure was chosen as the microwave flux concentrator because it did not support large eddy currents and its frequency independence allows the use of large sample volumes without the normal pulling present in high-Q cavities, which tends to broaden the resonance line.

A simple microwave bridge was used in the detection system (see Fig. 6). The klystron output was fed to the hybrid tee, which divides the power between the helix and the attenuator-phase shifter-short combination. The latter reflects a signal which is 180° out of phase with the reflection from the probe, and has suitable amplitude to bias the crystal detector to a low noise region. When

resonance occurs, the amplitude and phase of the reflected signal from the helix are modified, and the bridge is unbalanced. The resulting rf pulse sent to the crystal is amplified and presented to the vertical deflection plates of the oscilloscope.

Field Measurements in Quadrupole Magnets

The techniques used to measure such important parameters as magnetic center, length of the quadrupole field, harmonic content determination, and gradient measurement in quadrupole magnets will be discussed briefly.

Magnetic Center

In general, the magnetic center of a quadrupole magnet does not necessarily correspond to the mechanical center. In order to achieve proper alignment of the quadrupoles, the relationship of the magnetic center to the mechanical center must be known.

There are many methods of determining the magnetic center of a quadrupole, and three will be discussed here. Rotating coils provide one method. Because the field at the center of a quadrupole is zero, the output from an asymmetrical rotating coil is a minimum when the coil is at the center. Unfortunately, this method is difficult to use because one is trying to minimize the dipole field while the major contribution to the output of the rotating coils comes from the quadrupole field, which is not a function of position. This method can be useful, however, if one looks only at the amplitude of the dipole field. In this case, the amplitude of the field is completely a function of distance from the magnetic center, and the determination of position of the magnetic center is accurate to about ±0.001 inch.

A floating wire is another method of center determination for a quadrupole. This involves putting a taut wire through the magnet at the approximate center. First, the magnet is energized, then a current is passed through the taut wire, and deflection of the wire is noted as evidence that the wire is not at the magnetic center. The wire is then moved and the process repeated until no deflection of the wire is observed as the wire current is turned on. The wire is then in the magnetic center. The floating wire technique is probably good for center location to an accuracy of a few mils. For this type of accuracy, a considerable amount of elaborate equipment is necessary (temperature controlled, drift-free room, ripple-free power supplies).

The third, and in our case the most important method of magnetic center determination, is the use of a colloidal suspension of ferrous and ferric oxide particles.

This technique was proposed and used by R. M. Johson,[9] to locate the magnetic center of quadrupole fields. The physical mechanism of this method was explained recently[10] as scattering of polarized light on aligned colloidal particles in a quadrupole field. In this system, a small vial of the suspension is placed in the magnetic quadrupole field such that the mechanical center falls within the area of the vial. White plane-polarized light is directed through the vial of solution from one end of the magnet (Fig. 7). The observer at the opposite end of the magnet looks at the vial through a plane-polarizing analyzer so aligned with the polarizer of incoming light that complete cancellation of light should occur when the magnetic field is turned off. With the magnetic field turned on, complete cancellation does not occur except along two mutually perpendicular axes which cross at the magnetic center of the quadrupole. This can be observed very accurately with an alignment telescope, and the magnetic center can be referenced directly to the mechanical structure of the magnet. This is the method presently used to determine magnetic centers; its accuracy is better than 0.001 inch.

Effective Length

The effective length

$$\frac{\int \frac{\partial B}{\partial r}\, ds}{\left(\frac{\partial B}{\partial r}\right)_{max}}$$

of a quadrupole is one of its most important characteristics because it is used in the matrix element when calculating the beam dynamics in a magnetic lens system. In general, the effective length is a function of the radial position r from the magnetic axis of the quadrupole. One method of finding the effective length involves using normal mapping procedures and plotting the field at a point r as a function of the axial position z for $-\infty < z < \infty$, plotting this on a graph, and integrating the area under the curve from $-\infty$ to ∞. This area is divided by the maximum field, and thus the effective length of the dipole field L_B as a function of radial position is obtained. From this, using the formula

$$L_G(r) = L_B(r) + r\,\frac{\partial L_B(r)}{\partial r}$$

the length of the quadrupole field L_G is calculable.

A second and easier method of effective length determination involves the use of four coils rotating on a single shaft (see Fig. 8). Two of the coils are long compared to the field while two are located in the central field of the magnet. The outputs from the long and short coils add in a quadrupole field but exactly cancel in a dipole field. The total output sinusoidal wave from the long coils is divided down on a precision potentiometer and compared with the total output sinusoidal wave from the small coils. The phase of the

outputs is exactly the same because the large and small coils are built in the same plane. The two signals are thus compared until the divider potentiometer is set for complete cancellation of the signals. Cancellation is facilitated by inversion of one signal with respect to the other, so that when the signals are equal they appear as a null. Then, by measuring the ratio of the induced voltages and knowing the coil dimensions, the effective length of the quadrupole field is calculable. Using this technique an accuracy of about 0.1% is assured.

Multipole Content

One of the most important methods of evaluating a quadrupole magnet is determining the "purity" of its quadrupole field. In any quadrupole magnet there are some higher pole fields present; these fields, if sufficiently large, can affect the beam dynamics in the magnet. Naturally, the quadrupole field is much larger than other multipole fields, and some provision must be made to cancel or at least reduce the quadrupole field coefficient sufficiently so that its presence does not mask the other multipole coefficients. To measure the higher harmonics one can use a special asymmetrically wound rotating coil which is designed to minimize the contribution due to the quadrupole field while enhancing the contributions from the other multipoles.[11] The coil rotates at a fixed frequency synchronized to the A-C line. The output from the coil is Fourier-analyzed with a narrow bandwidth wave analyzer and the amplitude of each Fourier coefficient is noted. In this system, the Fourier coefficient corresponding to the frequency of rotation ω of the coil is the dipole field, the coefficient corresponding to frequency 2ω is the quadrupole field, the coefficient of frequency 3ω is the sextupole field, and so forth for higher fields. The rotating coil can be calibrated in multipole calibrating magnets of known field strength, or its response can be calculated for a given coil geometry. A block diagram of such a harmonic analyzer system is shown in Fig. 9.

Gradient Measurement

In order to measure the gradient field, one has to measure the magnetic field strengths at two points along the radial direction. For this measurement a differential Hall probe detector with two probes separated by a known distance is very adequate. The gradient can be measured to better than 0.1% when the probes are calibrated individually in a known field. An excellent review of other types of measurements can be found in Refs. 12 and 13.

List of References

1. R. H. Helm and W.K.H. Panofsky, "Beam dynamics of the Project M accelerator," M Report No. 201, Stanford Linear Accelerator Center, Stanford University, Stanford, California (1960).

2. S. Penner, "Electron beam-deflecting systems for the Monster," M Report No. 200-13, Stanford Linear Accelerator Center, Stanford University, Stanford, California (1960); and H. S. Butler and J. J. Muray, "Deflection magnet systems for the primary beam," M Report No. 297, Stanford Linear Accelerator Center, Stanford University, Stanford, California (1962).

3. R. H. Helm, "Effects of stray magnetic fields and rf coupler asymmetry in the two-mile accelerator with sector focusing," SLAC Report No. 20, Stanford Linear Accelerator Center, Stanford University, Stanford, California (1963).

4. R. H. Helm, "Misalignment and quadrupole error problems affecting the choice of multiplet type for sector focusing of the two-mile accelerator," SLAC Report No. 15, Stanford Linear Accelerator Center, Stanford University, Stanford, California (1963).

5. R. H. Helm, "Optical properties of quadrupole multiplets for sector focusing in the two-mile accelerator," SLAC Report No. 14, Stanford Linear Accelerator Center, Stanford University, Stanford, California (1963).

6. S. Penner, Rev. Sci. Instr. 32, 150 (1961).

7. J. K. Cobb, D. R. Jensen, and J. J. Muray, Internal Report, Stanford Linear Accelerator Center, Stanford University, Stanford, California (1963).

8. J. J. Muray and R. A. Scholl, "Dynamic field measurements with an EMR magnetometer in the pulsed beam switching magnet," SLAC Report No. 26, Stanford Linear Accelerator Center, Stanford University, Stanford, California (1964).

9. R. M. Johson, Internal Report BEV-687, Lawrence Radiation Laboratory, Berkeley, California (1961).

10. J. J. Muray (submitted to J. Appl. Optics).

11. W. H. Lamb, Jr., Report WHL-1, Argonne National Laboratory, Argonne, Illinois (1962).

12. B. de Raad, "Dynamic and static measurement of strongly inhomogeneous magnetic fields," Thesis, The Hague (1958).

13. A Septier, Advances in Electronics and Electron Physics, vol. XIV (Academic Press, New York, 1961).

Bibliography

1. R. H. Helm and W.K.H. Panofsky, M Report No. 201, Stanford Linear Accelerator Center, Stanford University, Stanford, California (1960).

2. S. Penner, Project M Report No. 200-13, (1960). H. S. Butler and J. J. Muray, M Report No. 297, Stanford Linear Accelerator Center, Stanford University, Stanford, California (1962).

3. R. H. Helm, SLAC Report No. 20, Stanford Linear Accelerator Center, Stanford University, Stanford, California (1963).

4. R. H. Helm, SLAC Report No. 15, Stanford Linear Accelerator Center, Stanford University, Stanford, California (1963).

5. R. H. Helm, SLAC Report No. 14, Stanford Linear Accelerator Center, Stanford University, Stanford, California (1963).

6. S. Penner, Rev. Sci. Inst. 32, 150 (1961).

7. C. Germain, Nucl. Instr. and Methods 21, 17 (1963).

8. B. de Raad, "Dynamic and static measurement of strongly inhomogeneous magnetic fields," Thesis, The Hague (1958).

9. P. Grivet, High Magnetic Fields (The M.I.T. Press and J. Wiley, Inc., Cambridge, Massachusetts, 1962).

10. J. L. Symonds, Rep. Propr. Phys. 18, 83 (1955).

11. R. H. Lovberg, Ann. Phys. 8, 311 (1959).

12. G. K. Green et al., Rev. Sci. Instr. 22, 256 (1951).

13. E. W. Fuller and L. U. Hibbard, J. Sci. Instr. 31, 36 (1954).

14. Taieb et al., Onde Elect. 35, 1076/1083 (1955).

15. M. Epstein and R. B. Schulz, IRE Trans. Electron Devices (Jan. 1961).

16. Ch. G. Dols et al., Rev. Sci. Instr. 29, 349 (1958).

17. J. P. McEvoy, Jr., and R. F. Decell, Rev. Sci. Instr. 34, 914 (1963).

18. J. Malecki et al., Acta Physical Polonica, vol. XVI, p. 151 (1957).

19. A. Bonanni and G. Saceroloti, Note No. 182, Comitato Nazionale per l'Energia Nucleare, Laboratori Nazionali, Frascati, Italy (1963).

20. J. L. Stahlke, Nucl. Instr. and Methods 17, 157 (1962).

21. O. E. Spokas and M. Danos, Rev. Sci. Instr. 33, 613 (1962).

22. R. H. Webb, Rev. Sci. Instr. 33, 732 (1962).

23. J. J. Muray and R. A. Scholl, SLAC Report No. 26, Stanford Linear Accelerator Center, Stanford University, Stanford, California (February 1964).

24. J. K. Cobb, D. R. Jensen, and J. J. Muray, Internal Report, Stanford Linear Accelerator Center, Stanford University, Stanford, California (1963).

25. R. M. Johson, Internal Report BeV-687, Lawrence Radiation Laboratory, Berkeley, California.

26. J. J. Muray (submitted to J. Appl. Optics).

27. W. H. Lamb, Jr., Report WHL-1, Argonne National Laboratory, Argonne, Illinois (1962).

28. A. Septier, Advances in Electronics and Electron Physics, vol. XIV (Academic Press, New York, 1961).

Acknowledgements

The authors are most grateful to Professor J. Ballam and Dr. R. Taylor of the Stanford Linear Accelerator Center for many helpful suggestions, and to Dr. B. Hedin of CERN for valuable discussions.

TABLE I

Type of Instrument	Accuracy	Maximum $\frac{dB(Gauss)}{dt(sec)}$ which can be measured	Output Signal (Typical)	Approximate minimum pulse length (half sinusoidal)	References	Field range (Gauss)
RC Integrator	$\geq 0.1\%$	$\approx 10^{16}$	1 volt	$\approx$ 1 μsec-1 msec	7, 8, 9, 10, 11	up to maximum fields
Miller Integrator	$\geq 0.1\%$	$\approx 10^{7}$	1 volt	μsec-dc	7, 8, 9, 10, 12	up to maximum fields
Voltage to frequency converter type Integrator	$\geq 0.1\%$	$\approx 10^{4}$	Not Applicable	msec-dc	8, 9, 13, 14	up to maximum fields
Peaking Strip	0.1% (±0.02 Gauss)	10^{5}	0.1 volt	0.1 μsec-dc	7, 8, 9, 10	10^{-2} - 10^{2}
Semiconductor Field Probes	$\approx 1\%$	$> 10^{11}$	1 V in 10 kG field	μsec-dc	7, 9, 12, 16, 17	milligauss to 10^{5} gauss
Faraday Effect	$\approx 1\%$	$> 10^{11}$	Depends on Equipment	μsec-dc	7, 9, 18, 19	10^{-5} - 10^{6}
Electron Magnetic Resonance	0.1%	$\approx 10^{10}$	10 mV	μsec-dc	7, 8, 9, 20, 21, 22, 23	10 - 10^{4}
Nuclear Magnetic Resonance	$\geq 0.01\%$		10 mV	dc	7, 8, 9, 10	

Figure Captions

1. Schematic layout of beam switchyard.
2. Geometry of bending magnet.
3. 3° bending magnet positioner.
4. Rotating coil and turning mechanism.
5. Measuring setup.
6. Diagram of the magnetic field measuring system.
7. Experimental arrangement.
8. Rotating coils method of effective length determination.
9. Block diagram of harmonic analyzer for multipole magnetic field spectroscopy.

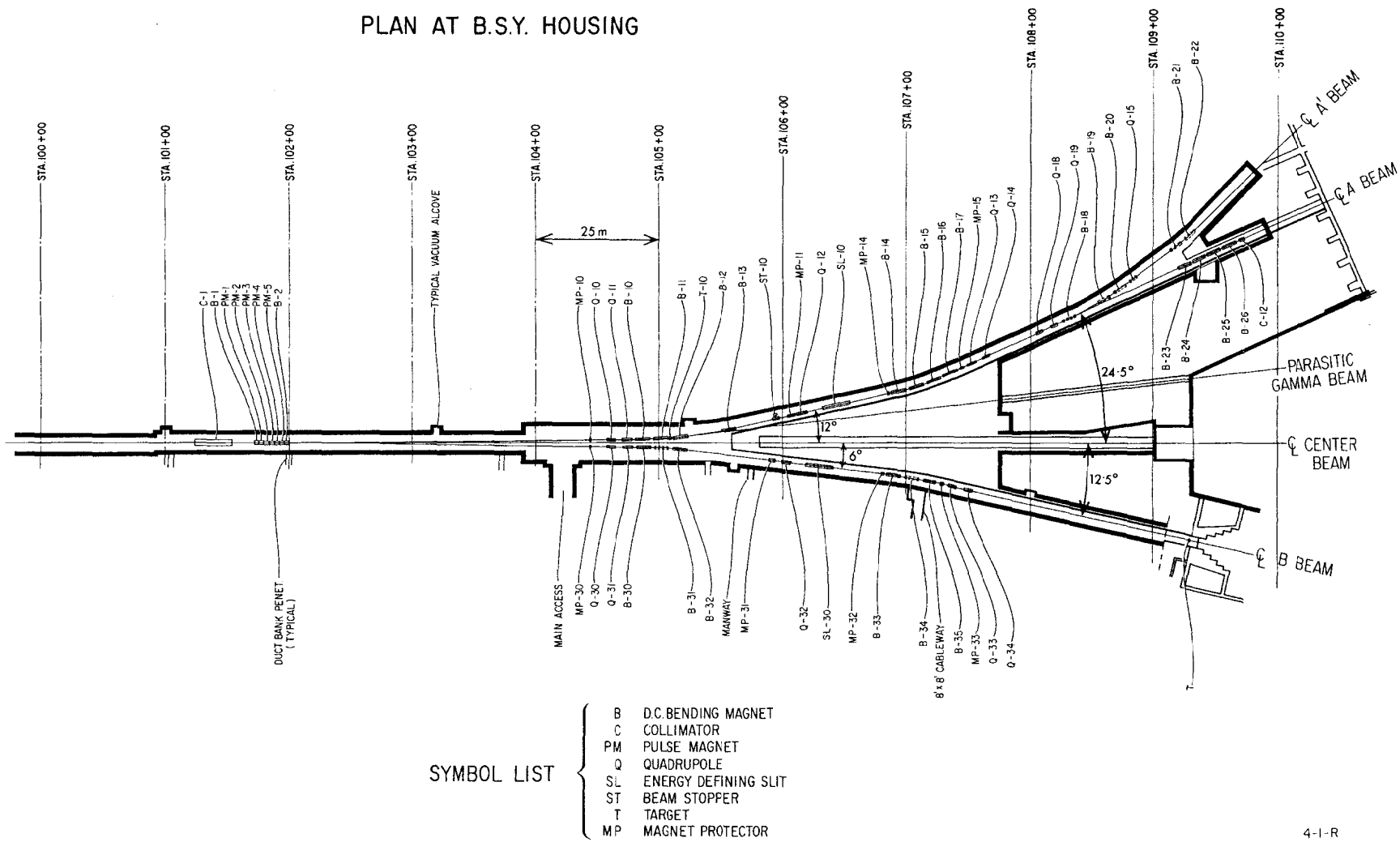

FIG 1. SCHEMATIC LAYOUT OF BEAM SWITCHYARD

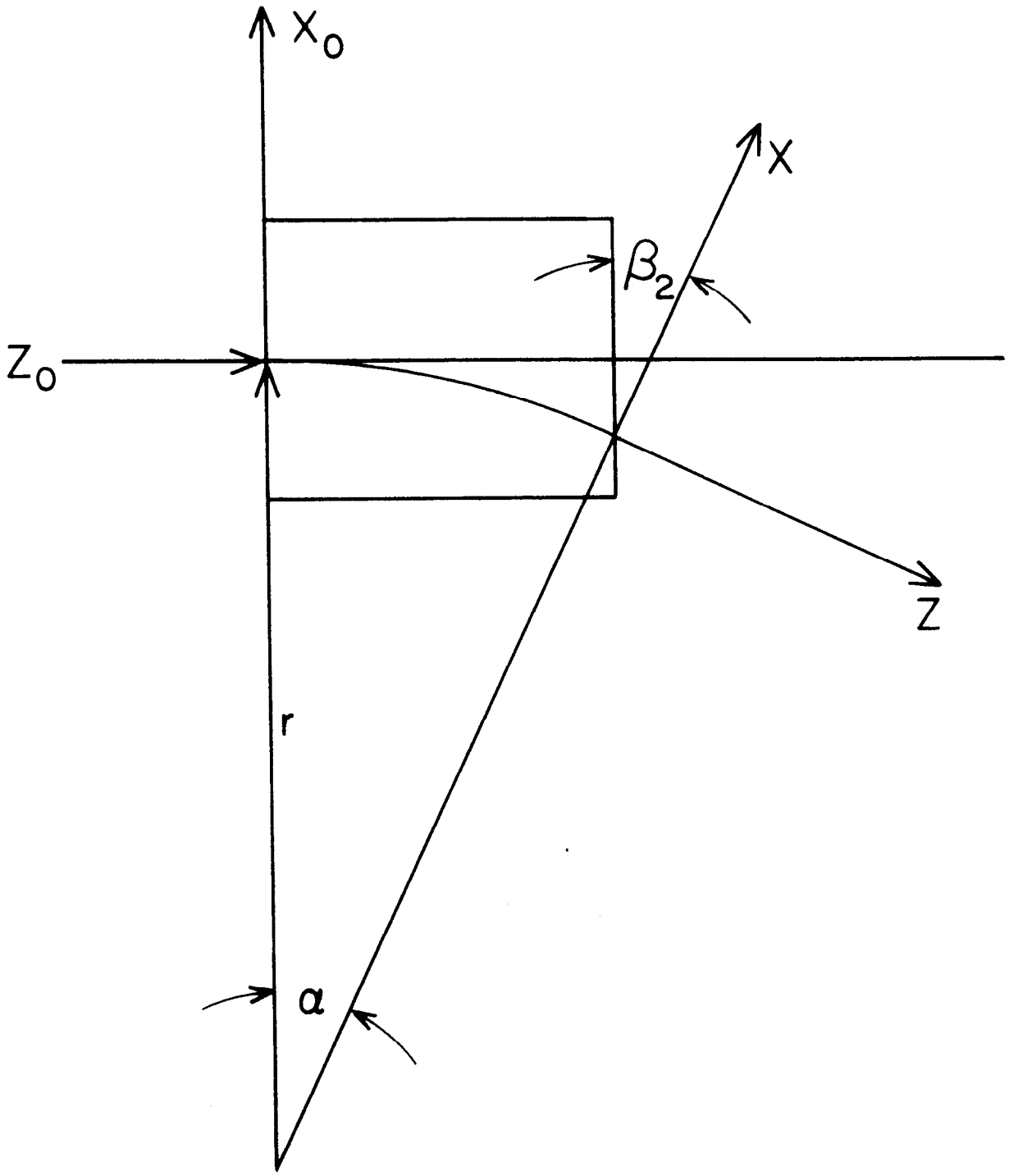

FIG 2. GEOMETRY OF BENDING MAGNET

168-1-A

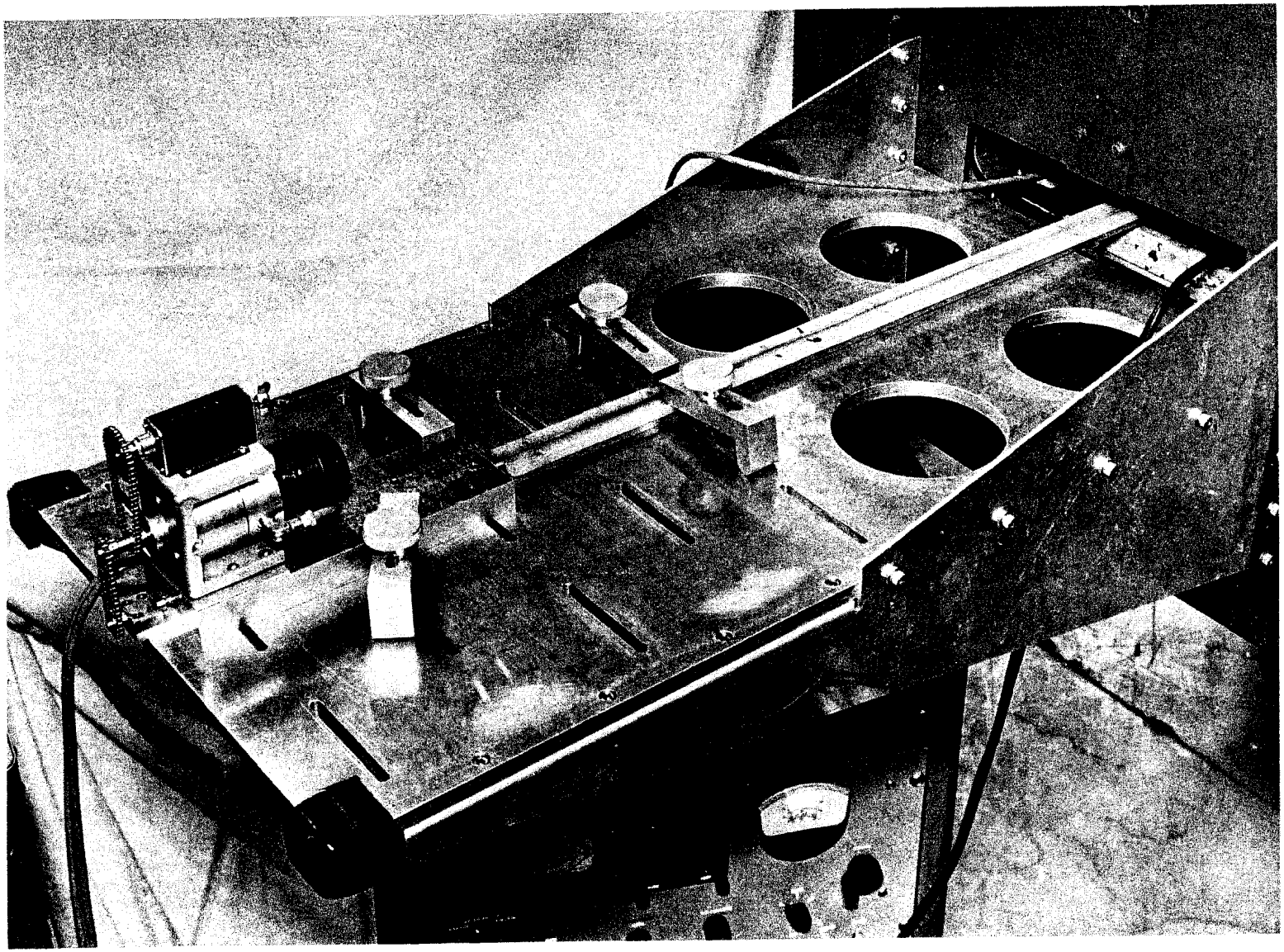

FIG 3. 3° BENDING MAGNET POSITIONER

FIG 4. ROTATING COIL AND TURNING MECHANISM

168-6-A

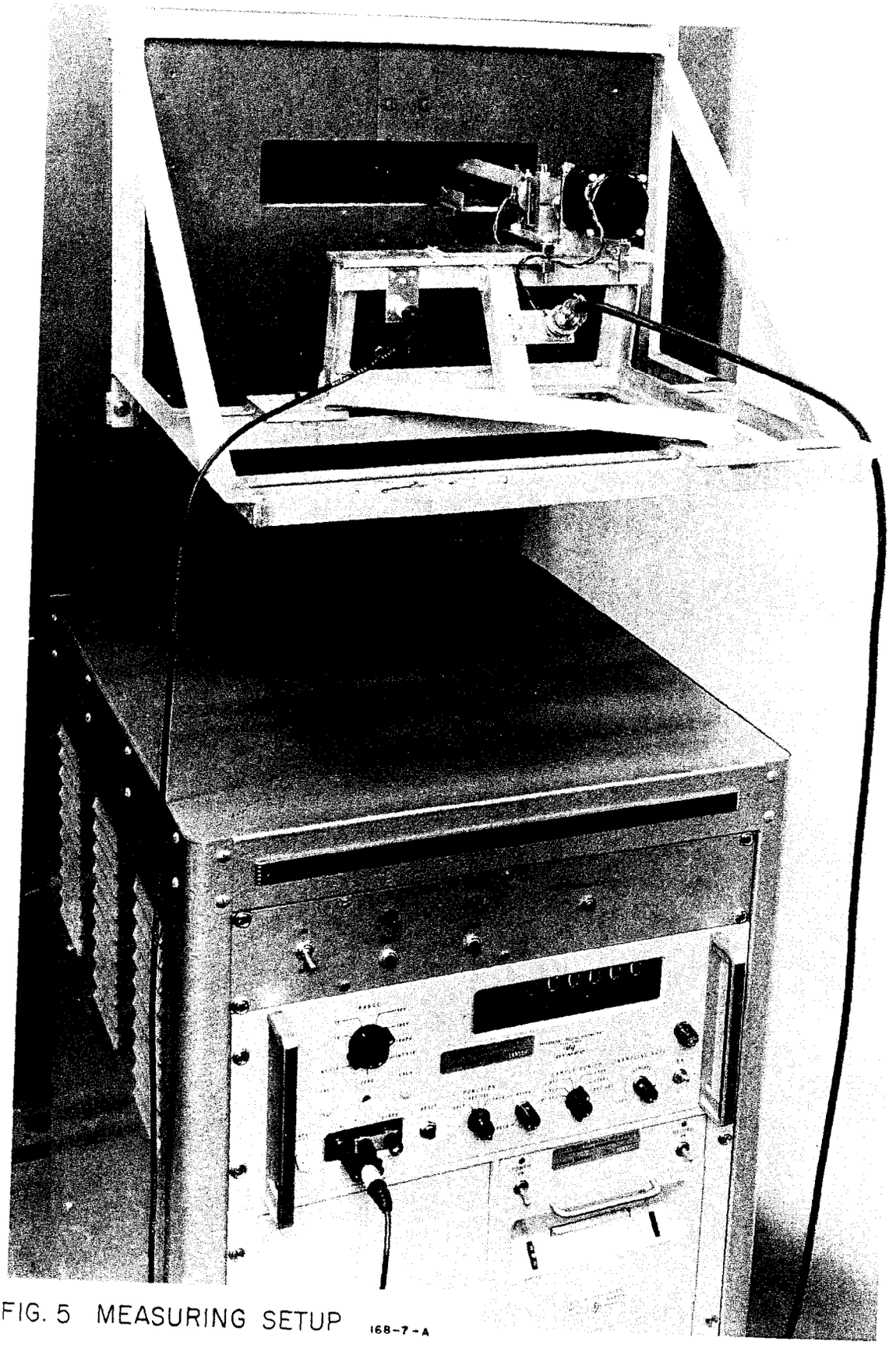

FIG. 5 MEASURING SETUP 168-7-A

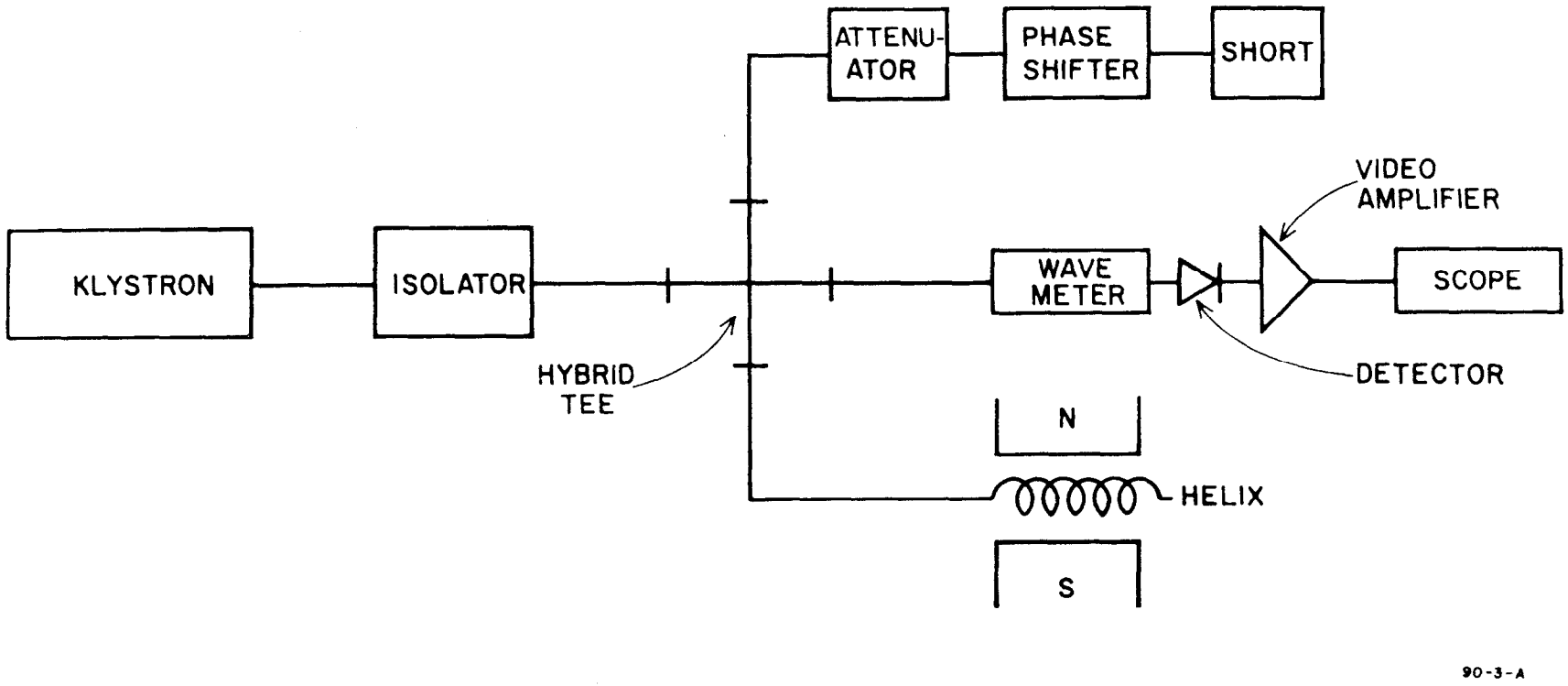

FIG 6. DIAGRAM OF THE MAGNETIC FIELD MEASURING SYSTEM.

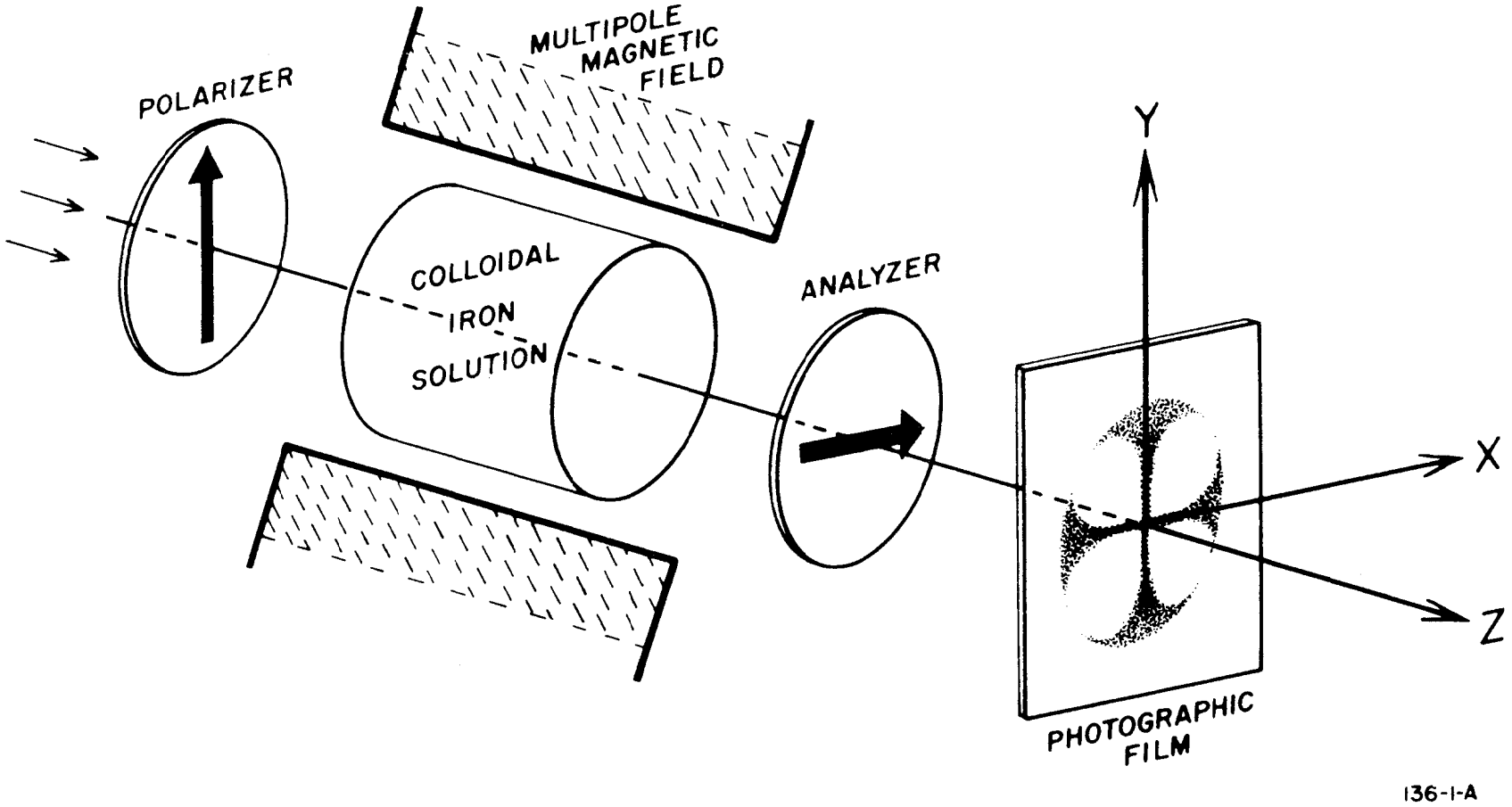
MULTIPOLE
MAGNETIC
FIELD
POLARIZER
COLLOIDAL
IRON
SOLUTION
ANALYZER
Y
X
Z
PHOTOGRAPHIC
FILM
136-1-A

FIGURE 7

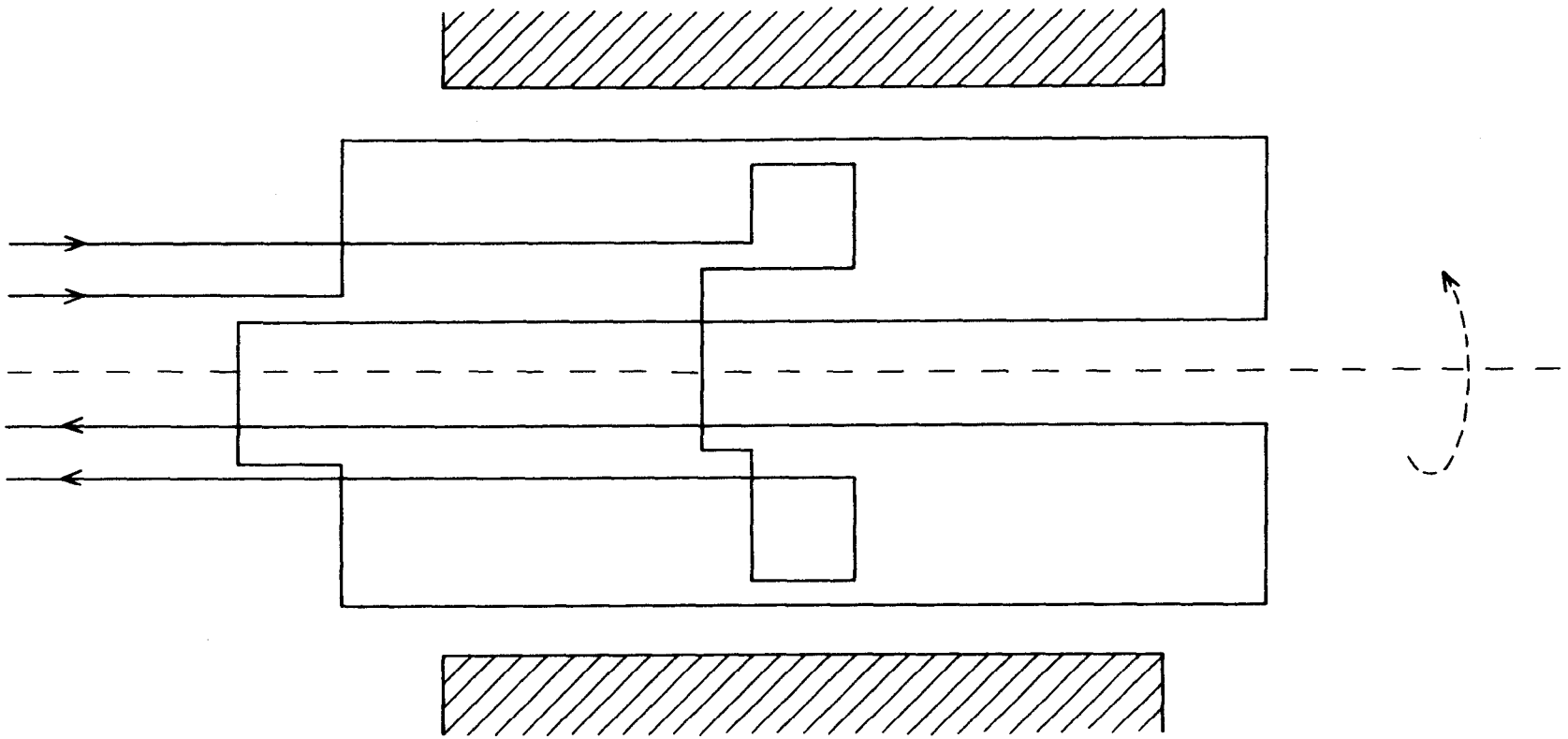

FIG. 8 ROTATING COILS METHOD OF EFFECTIVE LENGTH DETERMINATION

168-2-A

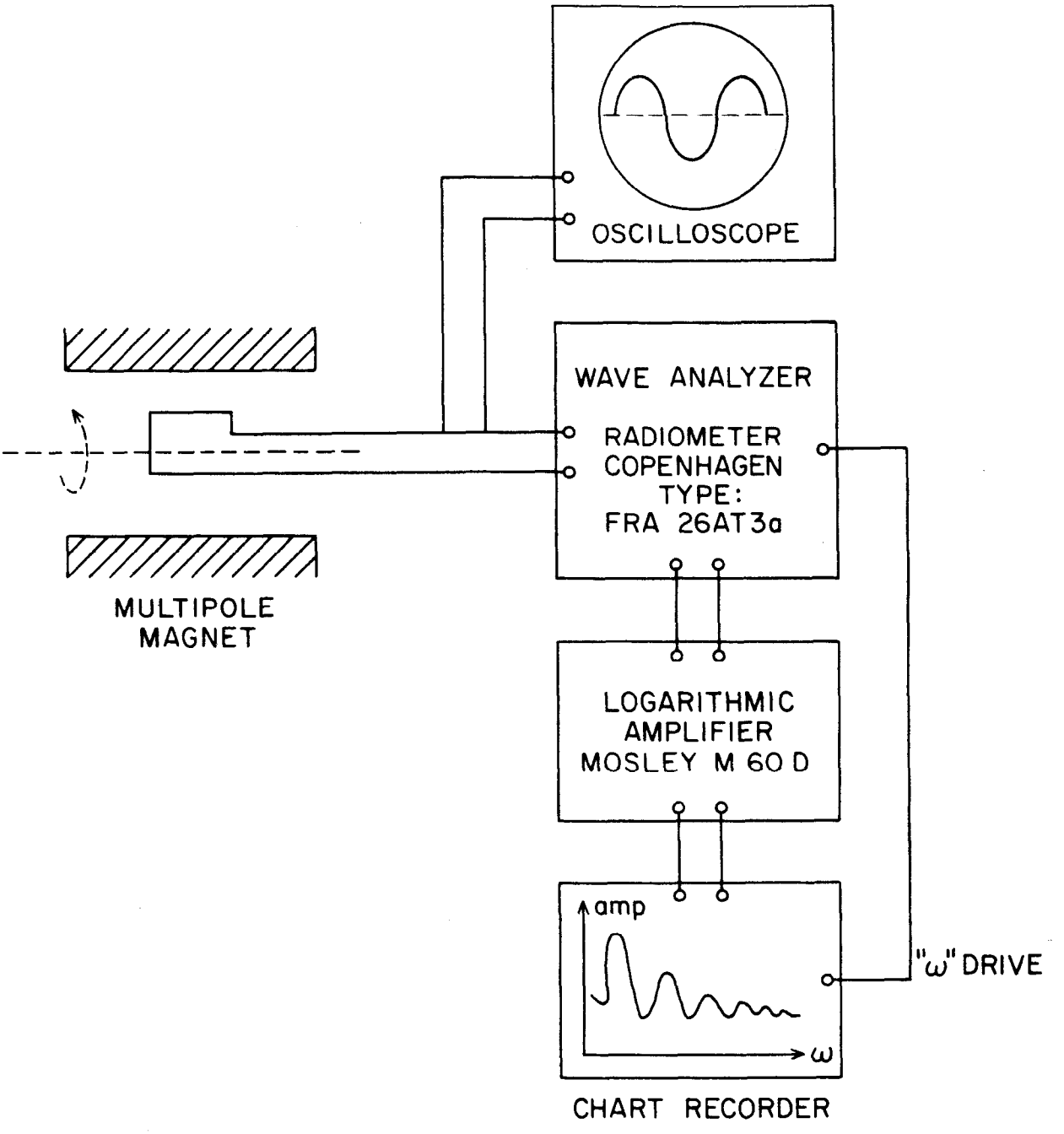

FIG. 9 BLOCK DIAGRAM OF HARMONIC ANALYZER FOR MULTIPOLE MAGNETIC FIELD SPECTROSCOPY

168-9-A